euspen's 21st International Conference & Exhibition, Copenhagen, DK, June 2021
www.euspen.eu

Design and manufacturing of deterministically micro-structured plates for capacitive sensors

Rudolf Meeß, Lars Daul, Stefan Verhülsdonk

Physikalisch-Technische Bundesanstalt (PTB), Bundesallee 100, 38116 Braunschweig, Germany

Rudolf.Meess@ptb.de

Abstract

Capacitive sensors are proven tools for high-resolution and high-precision distance measurements. Besides the properties and functionality of the electrical unit, the form deviations of the sensing surfaces, their alignment errors and the surface microtopography of these electrically charged surfaces influence the resolution and the precision of measurements. In this study, different deterministic microtopographies of sensing elements are simulated, manufactured and tested in a purpose-built setup. Aluminium plate electrodes with surrounding guard rings are manufactured with single-crystal diamond tools. The deterministic average roughness *Sa* is varied in the range of 74 nm to 626 nm. Furthermore, the experimental results are compared to the results of computational Finite Element Analysis (FEA).

Manufacturing, Ultra-precision, Design, Microstructure, Capacitive sensor

1. Introduction

Deterministic surface generation is used in many tasks for dimensional metrology. Roughness standards [1, 2], optical components made of glass or metal and many other surfaces depend on the highly repeatable structuring and patterning on the nanoscale. In this study, surfaces of capacitive displacement sensors are designed with respect to ultraprecise manufacturing procedures with single-crystal diamond tools, which have geometrically defined cutting edges.

The capacitive sensors consist of two circular metal plates, which form a parallel plate capacitor. One electrode is shifted against the other. The change in plate distance results in a change in electrical capacitance. This is converted into an electrical voltage using an AC measuring bridge. Each active electrode is enclosed by a guard ring, reducing the influence of stray capacitance and fringe fields at the edges. Both electrodes are adjusted in parallel, using an algorithm in which the nonlinearity of the displacement measurements is minimized. In this study, the gap size between guard ring and electrode is varied from 24 µm to 100 µm and the average roughness of the sensing surfaces is varied in the range from Sa = 74 nm to Sa = 626 nm. The sensor displacement is detected by an interferometric setup and thus can be evaluated. The complex experimental setup as a whole and the methodology will be reported elsewhere, and only meaningful partial results are presented here, concerning the influence of the manufacturing processes.

2. Manufacturing

For the turning operation, a Moore Nanotech 250UPL and for the planing a 650FG is used. Aluminium RSA905 of the RSP company is processed. The single crystal diamond tool has a nose radius of 5 µm with an arc of 60°. The rake angle is 0°. For the turning operation the spindle speed was kept constant to 2000 rpm. For the planing, feed was chosen to be 15.5 mm/min. The remaining parameters are shown in table 1.

In ultra-precision diamond turning and planing, the surface roughness is influenced mainly by the geometry of the tool and it's periodic replication. The theoretical total height of profile or roughness parameter *Rt* can be expressed as

$$Rt = r\left(1 - \sqrt{1 - \frac{f^2}{4r^2}}\right) \qquad (1).$$

The equation includes the tool nose radius *r* and the feed *f* as the feed per revolution. Besides this kinematic part, the elastic material spring back and the side flow, dynamic machining paramters, further plastic and inhomogenous material behaviour and finally thermal and geometrical machine errors can be included into a model [3]. In this study, these effects can be neglected.

The arithmetic surface roughness average *Ra* can then be integrated as a main function *z(x)* of the arc of the tool nose along the measured line l_R:

$$Ra = \frac{1}{l_r}\int_0^{l_r}|z(x)|dx \qquad (2),$$

or in Whitehouse's approximation [4]:

$$Ra \approx \frac{0.032\,f^2}{r} \qquad (3).$$

Table 1. Manufacturing paramters for electrodes. Spindle: 2000 rpm

Feed [mm/min]	**Feed f** [µm]	**Rt** [µm] *eq. [1]*	**Rt** [µm] *measurement*	**Ra** [µm] *eq. (3)*
5	2.5	0.16	0.25	0.04
7.5	3.75	0.37	0.52	0,09
10	5	0.63	0.67	0.16
15.5	7.75	1.5	1.5	0.38
20	10	2.5	2.5	0.64

The first values for the lower feed rates show a correlation of the calculated and measured roughness values of *Rt,* that is not so good. This is due to the sensitivity to single outliers in the range of 100 nm, which may not be avoided due to the sharp edges of the intersections of the resulting contour, see figure 1.

3. Results

Line scans of the different surfaces in table 1 are shown in figure 1. For the small amplitudes, no significant noise is visible in the amplitudes, while the large amplitudes of 2.5 µm vary by several percent.

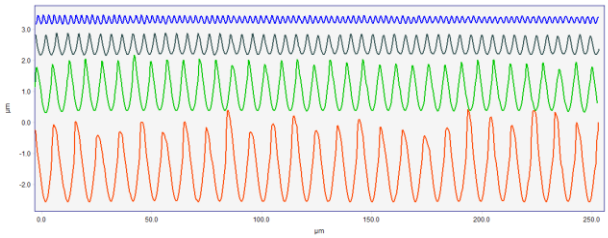

Figure 1. Linescans of turned probe surfaces with feeds *f* from top to bottom of 2.5 mm, 5 mm, 7.5 mm and 10 mm

A typical geometry of the manufactured gap between the guard ring and the plate is shown in figure 2. On the left, the topography is shown, as detected with the confocal laser scanning microscope Olympus LEXT4000. On the right, the plot along the extracted blue line is shown.

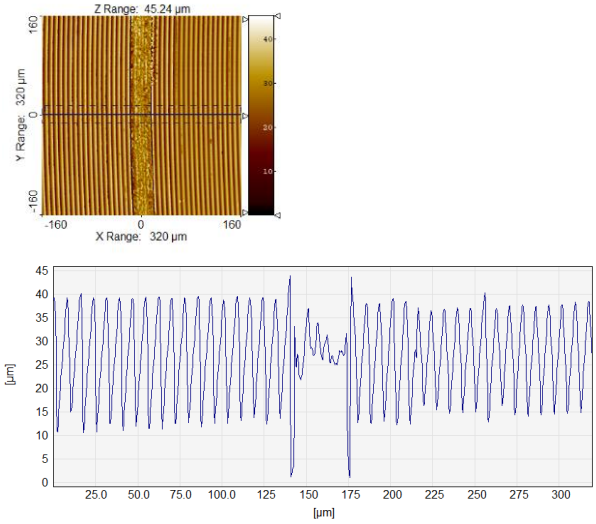

Figure 2. Topography of sensor: gap between target and guard ring

The adhesive between the parts is completely removed by the turning process and the burr at the edges of the aluminium is mild.

A correlating plot of the electrical surface-potential shows discrete rounded areas with significant lower potential on the aluminium planes. Kelvin Probe Force Microscopy mode (KPFM) of the AFM is used for this purpose. The detected islands cannot be correlated with dust or contamination on the topography plot. They are assumed to be due to the metallic composition of the aluminium alloy. X-ray analysis of the element composition and concentration on the surface delivered a discrete grain size distribution similar to the observed surface potential deviation.

The FEA (COMSOL Multiphysics) is based on charges in the half space. The roughness asperities are simulated as sinusoidal peaks opposite a plane.

It can be seen in figure 3, that in the simulation of the influence of roughness, the change of nonlinearitiy and the slope error are small for wavelengths up to 50 µm.

In the experimental investigation, the four electrodes with the topographies from figure 1 are shifted against an electrode in a range of up to 50 µm. The slope errors and nonlinearities against the interferometrically determined shift values are determined. The residuals of the four displacement measurements are compared. The result is shown in figure 4.

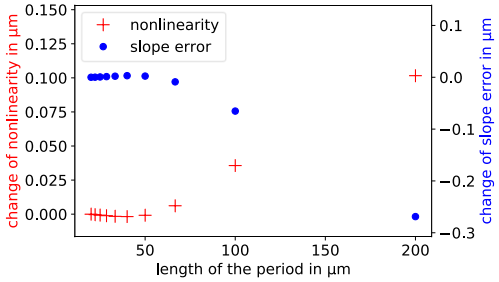

Figure 3. FEA results: Change of nonlinearity and change of slope as functions of length of period on probe surface. Amplitude: 5 µm

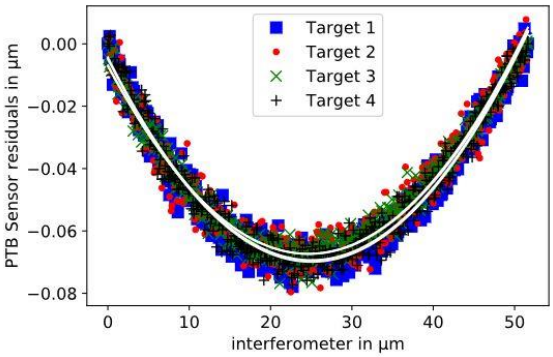

Figure 4. Measurement residuals of PTB capacitive sensor with different surface topographies as function of interferometrical distance signal

There is no measurable effect of surface roughness on the slope error and nonlinearity in this range. This is in good agreement with the results of the FEA.

4. Summary and Outlook

Several electrodes are manufactured for the characterization of capacitive sensors. Each electrode consists of two parts and it is assembled prior to ultraprecision turning and planing. Average roughness values are controlled in a range between 40 nm ≤ Ra ≤ 700 nm. It is shown in good agreement of simulation and experiment, which correlates the shift of the electrodes with a laser interferometer, that the effect of roughness can be neglected in the assessment of uncertainty in the shift up to 50 µm. In a next step, waviness will be applied to the active surfaces.

The influence of the machine and tool vibration will moreover be examined to attain a more exact prediction of the averaged and absolute roughness values.

References

[1] Meeß R, Felgner A and Verhülsdonk S 2020 Design and manufacturing of large range, discrete step chirp standards *Proceedings of the 20th international conference of the european society for precision engineering and nanotechnology* 399-402

[2] Meeß R, Hüser D, Jung-Albrecht L 2017 Analysis of geometrical errors in measurement data of ultraprecise-turned standards for roughness measurements *Proceedings of the 17th international conference of the european society for precision engineering and nanotechnology* 62-63

[3] He C L, Zong W J and Sun T 2016 Origins for the size effect of surface roughness in diamond turning *Int. J. Mach. Tools Manuf.* **106** 22–42

[4] Whitehouse D J 1994 Handbook of Surface Metrology (Institute of Physics) 649-660